The Soret Effect: A Review of Recent Experimental Results

Jean K. Platten

University of Mons-Hainaut,
Place du Parc, 20,
Mons 7000, Belgium

In the first part of the paper, we recall what the Soret effect is, together with its applications in science and industry. We emphasize the need to have a reliable data base for the Soret coefficient. Next we review the different techniques to measure the Soret coefficient (elementary Soret cell, beam deflection technique, thermal diffusion forced Rayleigh scattering technique, convective coupling and, in particular, the onset of convection in horizontal layers and the thermogravitational method). Results are provided for several systems, with both negative and positive Soret coefficients, and comparison between several laboratories are made for the same systems. We end with "benchmark" values of the Soret coefficient for some organic liquid mixtures of interest in the oil industry and to which all future new techniques should refer before gaining confidence. We conclude that correct values of the Soret coefficient can be obtained in earth conditions and we deny the need to go to microgravity. [DOI: 10.1115/1.1992517]

1 Introduction

The Swiss scientist Charles Soret discovered, in 1879, [1] that a salt solution contained in a tube with the two ends at different temperatures did not remain uniform in composition: The salt was more concentrated near the cold end than near the hot end of the tube. He concluded that a flux of salt was generated by a temperature gradient resulting, in steady-state conditions, in a concentration gradient. Although the German Ludwig [2] described the same phenomenon several years before in a one-page report, the name "Soret effect" is usually attributed to mass separation induced by temperature gradients because Soret studied the effect rather in details, formulated equations and finally wrote 3 or 4 papers on the subject [1,3,4]. Today one writes for the x component of the mass flux of the reference chemical compound in a binary mixture

$$\mathbf{J_x} = -\rho \mathbf{D}\frac{\partial \mathbf{c}}{\partial \mathbf{x}} - \rho \mathbf{D_T} \mathbf{c_0}(1-\mathbf{c_0})\frac{\partial \mathbf{T}}{\partial \mathbf{x}} \qquad (1)$$

The first term in the r.h.s. of Eq. (1) is Fick's law of diffusion, with c the mass fraction of the reference component and D the molecular (or isothermal) diffusion coefficient; the second term describes the Soret effect (or thermodiffusion effect), proportional to the temperature gradient $\partial T/\partial x$, with D_T the thermodiffusion coefficient. Since the effect does not exist in pure fluids one usually writes $c_0(1-c_0)$ factor of D_T. But as a matter of fact, D_T remains concentration dependant, exactly as D. Thus the second term in the r.h.s. of Eq. (1) describes mass separation due to a temperature gradient, whereas the first describes homogenization by normal diffusion. The two terms are thus of opposite sign, and when they are of equal intensity, we are in steady-state conditions $J_x=0$ implying

$$\frac{\partial \mathbf{c}}{\partial \mathbf{x}} = -\frac{\mathbf{D_T}}{\mathbf{D}}\mathbf{c_0}(1-\mathbf{c_0})\frac{\partial \mathbf{T}}{\partial \mathbf{x}} \qquad (2)$$

and the Soret coefficient is defined as

$$\mathbf{S_T} = \frac{\mathbf{D_T}}{\mathbf{D}} \qquad (3)$$

The Soret coefficient may be positive or negative depending on the sign of D_T or on the sense of migration of the reference component (to the cold or to the hot). In absolute value an order of magnitude for usual organic mixtures or aqueous solutions is $|S_T| \sim 10^{-3} - 10^{-2}$ K^{-1}.

According to Eq. (2), for a mixture containing 50 wt % of each component ($c_0 = 1/2$; $1-c_0 = 1/2$) and for a temperature difference ΔT of 4 K between hot and cold parts of the system, the difference in mass fraction Δc numerically will be equal to the Soret coefficient. Typically, Δc is of the order of 1%, sometimes smaller. But even if the separation remains small, the Soret effect has a lot of implications. Let us cite the operation of solar ponds [5], the microstructure of the ocean [6] since in both cases we have salty water and temperature gradients, and perhaps convection in stars [7]. The role of the Soret effect also has been evoked in biological systems, namely mass transport across biological membranes induced by small thermal gradients in living matter where thermodiffusion could assume a sizable magnitude for an ensemble of cells with the dimension of an organ or a tumor [8]. Another important application of the Soret effect is in natural hydrocarbon reservoirs [9,10]. One of the challenges in optimizing exploitation of oil reservoirs is a perfect knowledge of the fluid physics in crude oil reservoirs. Today, the modeling methods are based on pressure-temperature equilibrium diagrams and on gravity segregation of the different components of crude oil. However, improved models which more accurately predict the concentrations of the different components are necessary. The concentration distribution of the different components in hydrocarbon mixtures is mainly driven by phase separation and diffusion. One of the objectives in the oil industry is the prediction, as precisely as possible, of the gas-oil-contact in an oil reservoir. In order to achieve this goal, the local composition must be known. One of the reasons of a local compositional variation is molecular segregation in the gravitational field. Aside this important "force," the geothermal gradient (a few degrees per 100 meters) may also induce local variations in composition due to the thermodiffusion effect. In order to prove the implication of the Soret effect in crude oils, experiments in packed thermogravitational columns were undertaken by the group of Costesèque [11–14] on two samples of different origin: Alwijn and Oseberg, two oil fields in the North Sea. In packed thermogravitational columns we have two concentric cylinders kept at two different temperatures thanks to a flow of thermoregulated water. The space between the two

cylinders is filled with a porous medium, e.g., zirconium oxide spheres of given diameter. Next the porous medium is saturated by the mixture. The component that goes to the cold (resp. to the hot) cylinder under the effect of thermodiffusion is next advected to the bottom (resp. to the top) under the action of buoyancy. Thus a vertical concentration gradient for each component is built due to the interplay between Soret effect and convection. Samples are removed from two reservoirs at the top and at the bottom and analyzed. Even a simple inspection by eyes shows that the bottom sample is dark brown, whereas the top sample is almost clear indicating that the components belonging to the light fraction diffuse to the hot and are advected to the top; on the contrary the components of the heavy fraction diffuse to the cold cylinder. They also did a fine analysis by gas chromatography, analyzing the different isomers as, e.g., for hydrocarbons containing 8 carbon atoms: *n*-octane, 2-methylheptane, 3-methylheptane, 4-methylheptane, 2-2 dimethylhexane, 3-3 dimethylhexane, 2-3 dimethylhexane, 2-4 dimethylhexane, etc. They extended the analysis to all the isomers of ethyltoluene, trimethylbenzene, dimethylbutane, dimethylpentane, to meta-, ortho-, and paraxylene, and many more. In total 58 components were identified in the light fraction and analyzed. The same was done for the heavy fraction. By "analyzed" we mean that top and bottom concentrations (or mass fractions) of each component was determined. But in fundamental science, we need more than this. We need to quantify the Soret effect by "numbers." In Europe, there is a project initiated by the EGRT (European Group of Research in Thermodiffusion) with the aim to study a ternary system composed of dodecane (hereafter called C12), isobutylbenzene (IBB), and 1,2,3,4-tetrahydronaphtalene (THN). Results are in progress and all the 3 binaries were already investigated by 5 independent and different labs and results published [15]. But for ternary systems, there is no consent on the way to write the two independent fluxes, i.e., equations analogue to Eq. (1) and on the definition of the two independent Soret coefficients. Even in binaries, the measurement of the Soret coefficient defined by Eq. (3) remains delicate. Therefore, the paper is devoted to a summary of recent results that seem to us very safe, in contradistinction to the large discrepancies that are sometime observed in the literature, see [16] for an example, including recent microgravity determinations of S_T [17].

2 Some Different Techniques to Measure the Soret Coefficient

Arbitrarily we divide the different techniques into two groups: The first group supposes convectionless systems and Eqs. (1) and (2) apply; they are the correct working equations for the determination of the Soret coefficient. The second group of techniques uses convective coupling. We will mainly focus on this second group, simply because we made extensive use of these techniques. By the way these techniques will be different depending on the sign of the Soret coefficient we want to measure.

2.1 Convectionless Systems.

2.1.1 The Standard Soret Cell. A standard Soret cell (see Fig. 1) consists of two horizontal rigid plane plates, made of a good heat conducting material, e.g., copper or stainless steel. The plates are maintained at different temperatures by thermostatic circulating water in order to create a vertical temperature gradient in a parallelepipedic working space (there are of course lateral walls made of a poor heat conductivity material in order to minimize the heat exchange with the surroundings). The system usually is heated from above in order to avoid free convection. Between the plates a regular gap a is maintained by a brace made of, e.g., PVC into which small holes are managed (at least one, sometimes several in order to follow the kinetics of the separation). In each hole a watertight device is managed where curved hypodermic needles
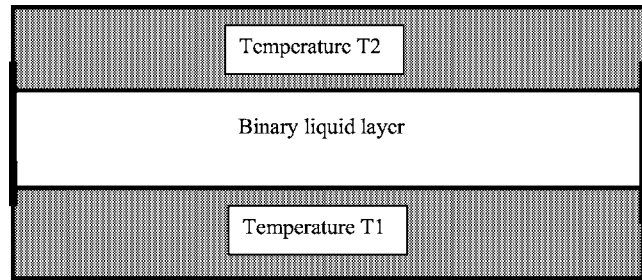

Fig. 1 Sketch of an elementary Soret cell

are inserted in order to remove very small liquid samples close to the isothermal horizontal boundaries. The samples are analyzed with a high resolution refractometer ($n\pm0.00001$) or densimeter ($\rho\pm0.000001$ gr/cm^3) in order to get the concentration difference Δc between the top and bottom removed samples after comparison with calibration curves. Next the use of Eq. (2) rewritten as

$$\Delta c = - S_T c_0 (1 - c_0) \Delta T \qquad (4)$$

gives S_T. Instead of considering ΔT as the temperature difference between the two bounding plates (or between the two thermostatic baths) it is much better to measure the local value of T (e.g., by thermocouples) at the exact location of the removed sample. Cells with 6 holes along the longer side are of common use [18] and at different times samples are removed in order to follow the time evolution of $\Delta c/\Delta T$ given by

$$\frac{\Delta c(t)}{\Delta T} = - S_T c_0 (1 - c_0) \left[1 - \frac{8}{\pi^2} \sum_{n \text{ odd}} \frac{e^{-n^2 \frac{t}{\theta}}}{n^2} \right] \qquad (5)$$

where θ is the relaxation time defined by

$$\theta = \frac{a^2}{\pi^2 D} \qquad (6)$$

Thus by considering the few first terms into the Fourier expansion (5), e.g., the first 5 terms, and by a curve fitting procedure to the experimental points $\Delta c(t)/\Delta T$, it is possible to get simultaneously $S_T = D_T/D$ (from the value of the separation at the steady state) and D (knowing the gap a between the two bounding plates). Thus as a byproduct, the thermodiffusion coefficient D_T is also determined.

2.1.2 The Beam Deflection Technique. The same type of cell as described in Sec. 2.1.1 is also used in the beam deflection technique [19–21], the main difference being that two opposite lateral walls are made of glass of good optical quality. The way to measure the mass fraction gradient is, however, totally different. Indeed in absence of any gradient, a laser beam perpendicular to one of the lateral glass wall will cross the liquid layer horizontally and hit the beam detection unit BDU at point A (Fig. 2). Due to the existence of vertical temperature and concentration gradients, a resulting index of refraction gradient will be created according
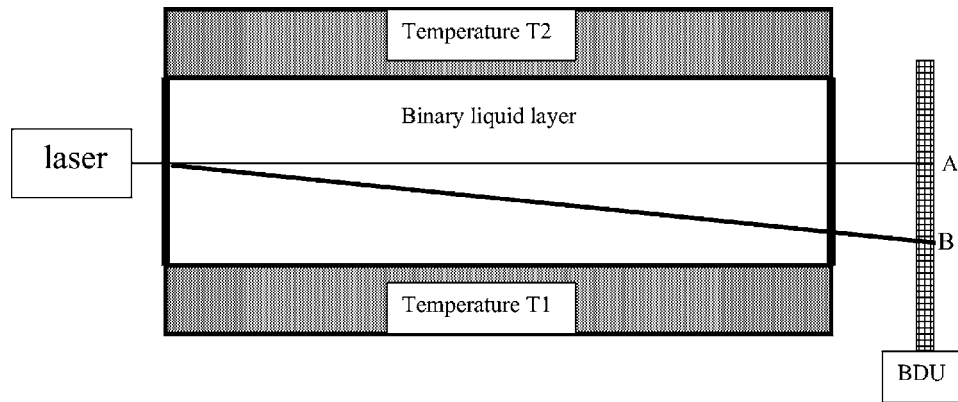
Fig. 2 Sketch of an elementary Soret cell using the beam deflection technique

to

$$\text{grad } \mathbf{n} = \frac{\partial \mathbf{n}}{\partial \mathbf{T}} \text{grad } \mathbf{T} + \frac{\partial \mathbf{n}}{\partial \mathbf{c}} \text{grad } \mathbf{c} \qquad (7)$$

In such a situation the laser beam, traveling in an index of refraction field, will not propagate horizontally, but will be deflected and hit the BDU at position B. The distance AB is a measure the deflection of the beam from which the index of refraction gradient may be deduced. Clearly two calibration curves are needed $\partial n / \partial T$ and $\partial n / \partial c$; finally (since the temperature gradient is known), the mass fraction gradient is deduced and produces the value of the Soret coefficient at the steady state. In addition one can make use of the very different relaxation times for the establishment of the temperature gradient and of the concentration gradient: Typically there are two orders of magnitude difference between both relaxation times since in liquids the diffusion coefficient is much smaller than the thermal diffusivity. Thus there is a quick process, the establishment of the temperature gradient just after the thermostatic baths are switched on, corresponding to a first fast variation of the index of refraction and a first deflection of the beam, followed by the slow process, the establishment of the concentration gradient. If one follows the kinetics of the second deviation of the beam, we have access to the diffusion relaxation time, thus to D and subsequently to D_T. Alternatively once the steady state is reached, one could switch off the two thermostatic baths: The temperature gradient is destroyed rather quickly, but the concentration gradient will take a longer time to disappear. Once again by following the time dependence of the deflection angle that has to return to zero, we may have the isothermal diffusion coefficient D.

2.1.3 The Thermal Diffusion Forced Rayleigh Scattering Technique (TDFRS). In the TDFRS technique [22], light is used to create the temperature gradient, instead of "boundary conditions." A first laser beam is split into two beams of equal intensity. The two beams emerging from the beamsplitter are focused by a lens in the sample containing the liquid mixture (Fig. 3(a)). At the intersection of the two laser beams, interference fringes are created (Fig. 3(b)) and by putting some chemically inert dye in the mixture a temperature grating is impressed, the temperature being higher (typically of 100 μK) in the fringe of high light intensity. And this periodic temperature field induces via the Soret effect a periodic concentration field. Both the temperature grating and the concentration grating create an index of refraction grating which is itself read out by a second laser by Bragg diffraction. The technique requires also two contrast factors $\partial n / \partial T$ and $\partial n / \partial c$ but will not work in the vicinity of a maximum of index of refraction as it is the case of some water-alcohol rich (90 wt %) systems. But this is also true for any technique that uses the index of refraction as a way to analyze the concentration gradient. In the

TDFRS technique, the characteristic length is the fringes spacing, i.e., $\sim 10~\mu$m. Therefore, the temperature gradient is of the order of 1 K/cm, as in more classical techniques where the gradient is imposed by circulating water baths. A clear advantage of the TDFRS technique is the small relaxation time: Since the characteristic length is 1 μm, the characteristic diffusion time will be of the order of $1-10$ milliseconds, instead of several hours with cells of ~ 1 cm size. However, in the TDFRS technique the experiment must be repeated many times (e.g., 5000) and the results are averaged. The possible role of convection has been discussed in [22] showing that correct results are obtained by this technique.

2.2 Convective Coupling. In all convective coupling techniques, the idea is to study the modification of the velocity field (the pattern, the amplitude or the onset of convection in certain circumstances) under the effect of thermodiffusion. Therefore, the important parameter is the solutal contribution to the buoyancy force $\delta \rho . g$. We need an equation of state for the density and ignoring nonlinear terms we take
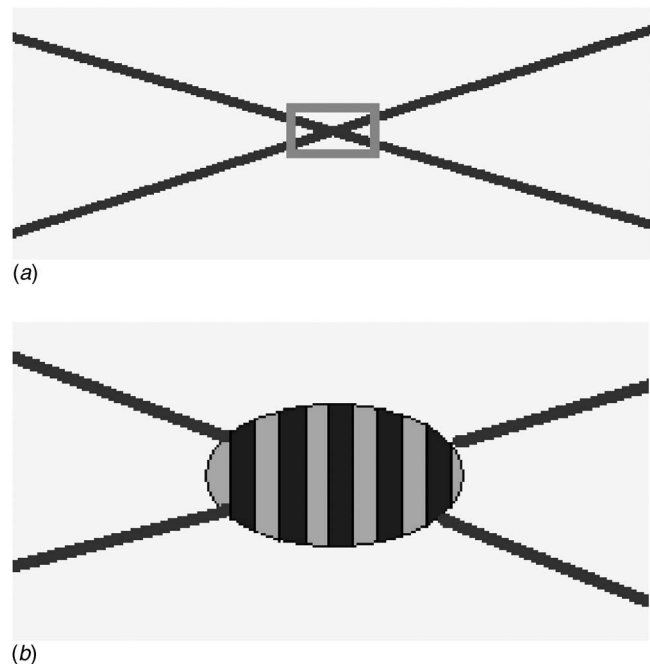

(a)

(b)

Fig. 3 Crossing of the beams in the sample (a) and zoom on the fringes (b) in the TDFRS technique
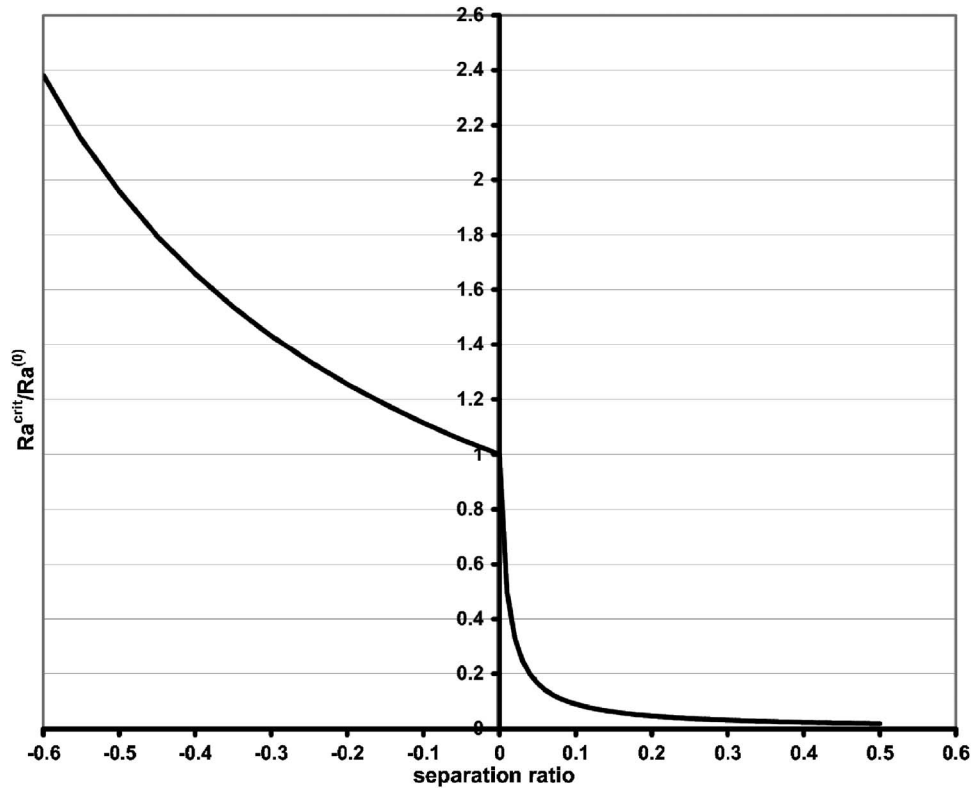
Fig. 4 Variation of the critical Rayleigh number in the Rayleigh-Benard configuration as a function of the separation ratio

$$\rho = \rho_0[1 - \alpha(T - T_0) + \beta(c - c_0)] \quad \alpha > 0;\ \beta > 0 \qquad (8)$$

where α is the thermal expansion coefficient and β the mass expansion coefficient. They are both defined positively, because we decide (arbitrarily) that c represents the mass fraction of the heavier component. Of course the opposite choice could equally be made without affecting the physical results. T_0 and c_0 are reference temperature and mass fraction (mean values). As written before, the important parameter is the solutal contribution to the buoyancy, but relative to the thermal contribution. This parameter is called the "separation ratio" Ψ and, using Eq. (4) can be written as

$$\Psi = \frac{\beta \Delta c}{-\alpha \Delta T} = \frac{\beta}{\alpha} S_T c_0 (1 - c_0) \qquad (9)$$

2.2.1 Rayleigh-Benard Configuration. In the classical Rayleigh-Benard configuration, the monocomponent horizontal liquid layer is heated from below, inducing a potentially unstable density gradient: Convection sets in provided the Rayleigh number overcomes some critical value $Ra^{(0)}$ with a numerical value depending on boundary conditions ($27\pi^4/4$ or 1708 or…). We shall not enter here into the details of this well known hydrodynamic stability problem [23]. For a binary liquid layer in the presence of the Soret effect, two cases must be considered depending on the sign of the separation ratio. If Ψ is positive, thermal and solutal contribution to the buoyancy are of the same sign and since the thermal contribution is destabilizing (we heat from below) so is the concentration gradient; in other words the denser component migrates to the cold upper boundary, and this is a destabilizing process; the onset of convection will appear for a temperature difference (or a Rayleigh number) much smaller than that for a pure fluid system. If Ψ is negative, thermal and solutal contributions are of opposite sign and since the thermal contribution is destabilizing, the concentration gradient is stabilizing: the

denser component migrates to the hot lower boundary and the onset of convection is delayed to a temperature difference (or Rayleigh number) much greater than that for a pure fluid system. This is what Fig. 4 shows, but one recognizes immediately that the two curves for negative and positive separation ratio are quite different: They correspond to a different mode of instability. When Ψ is negative, we have an inverted Hopf bifurcation and instability arises as oscillations of increasing amplitude. The linear hydrodynamic stability theory gives the variation of the critical Rayleigh number as a function of the separation ratio see, e.g., [24] for a small review

$$\frac{Ra^{crit}}{Ra^{(0)}} - 1 = 1.15 \frac{-\Psi}{1 + \Psi + \dfrac{1}{Pr}} \qquad (10)$$

and the Hopf frequency as well

$$\omega = 1.43 \frac{3\pi^3}{2} \sqrt{\frac{-\Psi}{1 + \Psi + \dfrac{1}{Pr}}} \qquad (11)$$

In these two last equations, Pr is the Prandtl number $Pr = v/\kappa$ where v is the kinematic viscosity and κ the thermal diffusivity $\kappa = \lambda/\rho C$ (λ: thermal conductivity and C mass specific heat). Thus an indirect way, but nevertheless a not less precise way to determine a Soret coefficient, is to measure the critical Rayleigh number and the associated Hopf frequency. Therefore, we need to detect the onset of free convection as precisely as possible, together with a time record of the velocity each 2 s in order to deduce the Hopf frequency. This is achieved by Laser Doppler Velocimetry and with equipment specially dedicated to measure extremely low velocities, down to $5–10\ \mu m/s$. In Fig. 5 we show an example of the oscillatory onset of free convection that was recently obtained [25]. The experimental conditions are the fol-
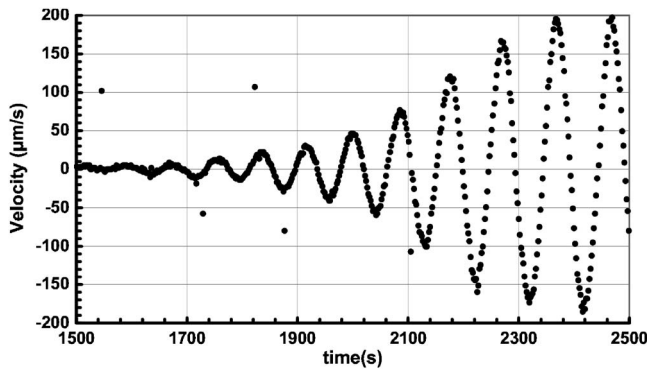
Fig. 5 Oscillatory onset of convection at $\Delta T = 1.84\,^{\circ}\text{C}$ in the system water (90 wt %)–isopropanol (10 wt %). Mean temperature: 21 °C.

Table 1 Comparison of the Soret coefficient of the system water (92 wt %)–ethanol (8 wt %) obtained in different laboratories

From Rayleigh-Benard experiments [18]	Kolodner [13]	Zhang [14]	Bou-Ali et al. [20]
$-7.08 \ 10^{-3} \ \text{K}^{-1}$	$-7.13 \ 10^{-3} \ \text{K}^{-1}$	$-7.30 \ 10^{-3} \ \text{K}^{-1}$	$-7.05 \ 10^{-3} \ \text{K}^{-1}$

lowing: The working fluid is a mixture of water (90 wt %) –isopropanol (10 wt %) in a parallelepipedic container of large lateral extension compared to the fluid thickness (4.75 mm) and comparable to Fig. 1, except that we heat from below; the temperatures of the lower and upper bounding plates is thermoregulated and the difference ΔT increased very slowly (mean value: 21 °C). After each temperature increase, we wait five times the relaxation time, i.e., in the present case 8 h. Near the critical point, ΔT is increased by steps of 0.1 °C for a rough determination of the critical Rayleigh number and by steps of 0.01 °C for a precise determination; below $\Delta T = 1.84\,^{\circ}\text{C}$ we have the rest stat, even after 8 h. When ΔT is increased up to $\Delta T = 1.84\,^{\circ}\text{C}$, convection sets in; however, we have to wait 1700 s after the last increase of ΔT before to record for the first time measurable velocity amplitudes. In Fig. 5 an experimental point is taken each 2 s. Thus from Fig. 5 we have two informations: The critical temperature difference for the onset of free convection from which the critical Rayleigh number may be computed provided we have accurate values of the viscosity and of the expansion coefficient, but this is usually not a problem (see later), and the Hopf frequency from the Fourier transform of the time signal $V(t)$ for small times, say between 1700 s$<t<$2300 s; for $t>$2300 s, when the amplitude of the velocity increases such that the nonlinear terms cannot be ignored in the theory, there is a gradual change in the frequency (or in the period); the final frequency, corresponding to nonlinear traveling waves differs from the Hopf frequency by one order of magnitude. Having the critical Rayleigh number and the Hopf frequency, we make use of Eqs. (10) and (11) to deduce the separation ratio Ψ and next S_T, having the two expansion coefficients α and β (and once again this is not a problem, see later). If the two values do agree within say a few %, then we may have confidence in the technique. Moreover having two values for S_T, we take their mean to compare with other values found in the literature. This comparison exercise has been made for several systems in [24]. The water (90 wt %)–isopropanol (10 wt %) system is spectacular because of its large Soret coefficient (and thus Hopf frequency) and that is why we did choose this system for showing Fig. 5 as an example, but this system is not popular (besides ourselves, only one other lab did investigate this system). Therefore, for a comparison between several labs the system water (92 wt %)–ethanol (8 wt %) at 25 °C is more appropriate. Table 1 gives a comparison between four different labs that use different techniques and clearly the use of the onset of convection in a Rayleigh-Benard experiment produces results in complete agreement with other techniques.

Since the onset of free convection seems a convenient way to measure negative Soret coefficients, we may think about using it for positive values. There are two reasons why this will not work. First, the bifurcation is forward and "normal;" thus we lose the possibility given by the Hopf frequency to have an additional experimental value of the Soret coefficient in the same experimental session. But moreover as shown by Fig. 4 there is a drastic drop in the critical Rayleigh number and Eq. (10) cannot be used because the instability mode is different. The variation of the critical Rayleigh number for positive values of the separation ratio is of the type

$$\text{Ra}^{\text{crit}} = \text{Ra}^0 \frac{1}{1 + \Psi(\text{Le} + 1)} \qquad (12)$$

where Le is the Lewis number defined by Le$=\kappa/D$. Since in liquids the thermal diffusivity κ is two orders of magnitude larger than the mass diffusivity D, Le$\sim$100 and even for the modest value $\Psi = +0.2$ (the solutal contribution to the buoyancy force is only 20% of the thermal contribution), there is a typical decrease of a factor 20 in the Rayleigh number, thus in the temperature difference needed to promote convection. For a layer of a few mm thick (say 4 mm) the critical temperature difference for pure water is of the order of 2 °C, a convenient value that can be measured accurately using commercial thermostatic baths. The addition of alcohol (such that S_T becomes positive) lowers the temperature difference by a factor 20 down to 0.1 °C. In other words we totally lose accuracy. Therefore, for positive Soret coefficients the onset of free convection is not the appropriate way to measure a Soret coefficient unless the temperature of each bounding plate is controlled at the 0.001 °C level, which was not the case in our experiments. Consequently we use another strategy: The thermogravitational process.

2.2.2 The Thermogravitational Process. A thermogravitational column usually consists of two vertical concentric cylinders at two different temperatures in such a way to create a horizontal temperature gradient. For reasons explained later, we prefer the use of parallelepipedic columns made of two rigid vertical copper plates A (see Fig. 6 and [27]) maintained at two different temperatures by circulating water in circular cavities B managed in each plate (only shown for the left plate in Fig. 6). The gap between the two plates is fixed and imposed by spacers C and D. In the upper spacer D there are two small holes for the filling of the column and for air to escape during the filling. Along the column height 5 sampling taps allow to remove with a syringe small quantities (1 and 2 ml) of the liquid, next analyzed to find their composition. Indeed, since the temperature gradient is horizontal, under the action of the Soret effect one of the components goes to the left (or to the cold plate) and the other to the right (the hot plate). The component that thermodiffuses to the cold is advected to the bottom, and the one that goes to the hot is advected to the top of the cell. Thus the combined effect of thermodiffusion and convection finally creates a vertical mass fraction gradient, resolved by the sampling process. Finally in order to close the space available to the liquid we need front and back windows. We used windows made of glass of good optical quality in order to have optical access in the column. Using once again LDV, we may follow the time evolution of the velocity amplitude. Combined to the vertical mass fraction gradient, we have two informations related to the Soret coefficient from two separate experiments (that usually are made at different times).

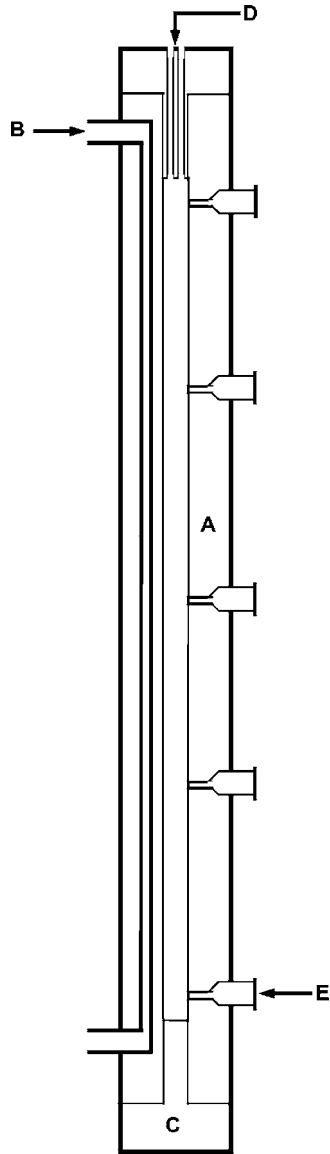The removed samples at the five sampling positions are ana-

Fig. 6 Sketch of the thermogravitational column

Fig. 7 Density profile in the thermogravitational column in the system water (60.88 wt %) – ethanol (39.12 wt %). $T_{cold}=20$ °C; $T_{hot}=25$ °C.

lyzed by measuring their density (the index of refraction could equally work well) using the quartz U-tube vibrating densimeter manufactured by Paar (DMA5000) having a resolution of 10^{-6} gr/cm³. Figure 7 shows a vertical mass fraction profile for the system water (60.88 wt %) – ethanol (39.12 wt %), a system that has been investigated by several labs. The linearity of the profile seems perfect. Of course we have to transform density into mass fraction. To this end we prepared 13 samples around 60.88 wt % of water, namely between 58 and 64 wt %, by steps of 0.5 wt % taking for each prepared sample the density, Fig. 8. This is our calibration curve giving also the mass expansion coefficient β needed in the separation ratio, the relevant parameter when measuring velocity amplitudes. Combining Figs. 7 and 8, we have the mass fraction profile, in particular the mass fraction difference between the top and the bottom of the column. We need of course a correct working equation giving the thermodiffusive coefficients from the knowledge of this mass fraction difference. This equation is derived from the Furry-Jones-Onsager theory, modified by Majumdar for concentrated solutions [28–31]. Since this theory is more than half a century old, we do not feel the necessity to explain it here. Let us simply stress that the equations can be simplified when the gap between the two lateral walls of the col-
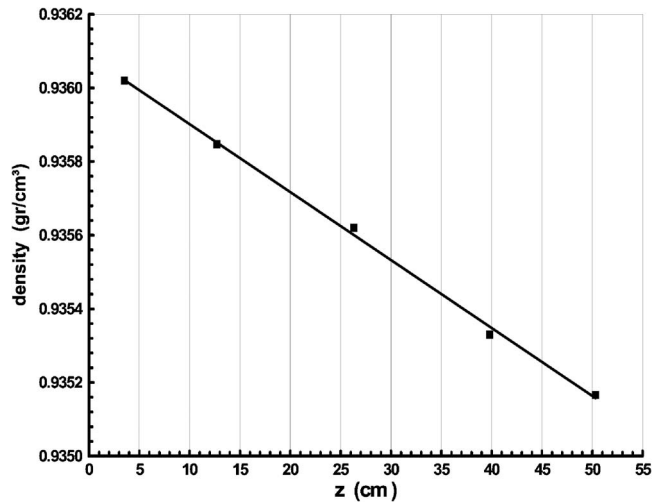
umn is "large," in practice for most of organic liquid mixtures, larger than 1 mm, but this is actually the case. The working equation then reads:

$$\Delta c = c_{bottom} - c_{top} = 504 \frac{\nu}{\alpha g} D_T c_0 (1 - c_0) \frac{H}{e^4} \quad (13)$$

where ν is the kinematic viscosity (the dynamic viscosity is measured for each system that we investigated by a falling ball Höppler viscosimeter, instead of trying to interpolate between values found in tables), H the height of the column ($H=530$ mm), e the gap ($e=1.58$ mm), and α the thermal expansion coefficient. This last parameter is determined by measuring the density of the initial sample at different temperatures as shown in Fig. 9 between 21 and 24°C, since the mean working temperature was 22.5°C ($T_{cold}=20$°C; $T_{hot}=25$°C). Let us mention that due to the simplifications made in the theory for "large gap," the temperature difference ΔT between the two walls no longer appears in Eq. (13); this is of course not true for the "small gap," theory for which Δc is an increasing function of ΔT. We now do possess all the necessary information to deduce from Eq. (13) the thermodiffusion coefficient D_T. But what we search is the Soret coefficient $S_T = D_T/D$. Therefore, we have to find in a supplementary and independent experiment the value of the isothermal diffusion coefficient D. This is achieved by the open ended tube technique [32], see Fig. 10. A small tube containing say the solute and the solvent is immersed at time $t=0$ in a container of very large volume compared to that of the tube and containing only the solvent. The system is of course at constant temperature by a circulating water flow and is covered to avoid evaporation. The solute diffuses outside of the tube and is not supposed to change the composition of the bulk because of its large volume. Instead of having pure solvent in the bulk and solvent+solute in the tube, the method works equally well with a mixture of two components in the bulk and in the tube, having, however, different mass fractions differing only by a few wt % around the initial mass fraction of the mixture for which we seek D_T and D (one should take care that the mixture in the tube has a density slightly higher than in the bulk to avoid free convection currents). The diffusion of the more concentrated component in the tube obeys Fick's law of diffusion

$$\frac{\partial c}{\partial t} = D \frac{\partial^2 c}{\partial z^2} \quad (14)$$

Subjected initial and boundary conditions ($c=c_0$ $\forall z$ at $t=0$; $\partial c/\partial z=0$ at $z=0$ and $c=c_\infty$ at $z=L$ for $t>0$, where c_∞ is the con-
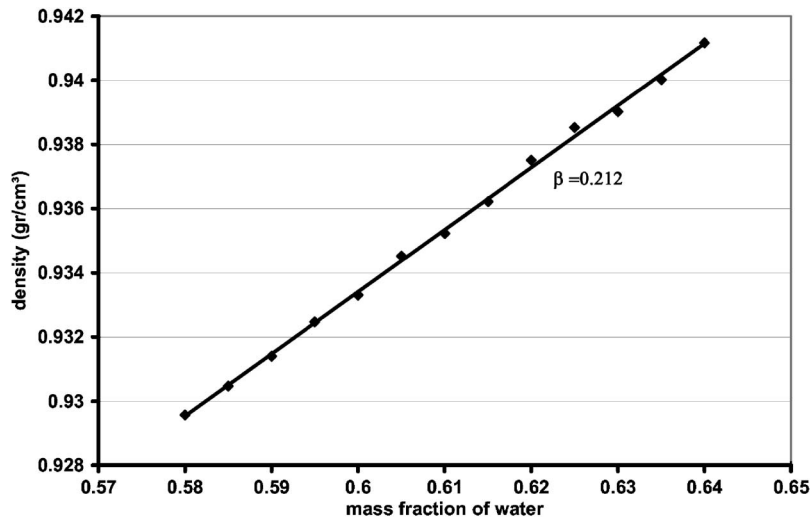
Fig. 8 Mass expansion coefficient in the system water (60.88 wt %) –ethanol (39.12 wt %)

centration of the bulk supposed to be of "infinite" volume and, therefore, of constant composition), the solution of Eq. (14) is

$$\mathbf{c(z,t)} - \mathbf{c_\infty} = \frac{4}{\pi}(\mathbf{c_0} - \mathbf{c_\infty})\sum_{\mathbf{n=0}}^{\infty} \frac{\sin\left[\left(\mathbf{n}+\frac{1}{2}\right)\pi\frac{\mathbf{z}}{\mathbf{L}}\right]}{\mathbf{2n+1}}\mathbf{e}^{-(\mathbf{n}+1/2)^2(\pi^2/\mathbf{L}^2)\mathbf{Dt}}$$

(15)

After a sufficiently long time (depending of course on $\mathbf{D}/\mathbf{L}^2$), typically 24–48 h, the leading term $n=0$ in the Fourier expansion is far sufficient to describe the time evolution of the average tube concentration $\langle\mathbf{c(t)}\rangle=1/\mathbf{L}\int_0^{\mathbf{L}}\mathbf{c(z,t)dz}$ and its decay is exponential. Thus the working equation for deducing D is

$$\ln\left(\frac{\pi^2(\langle\mathbf{c(t)}\rangle - \mathbf{c_\infty})}{8(\mathbf{c_0} - \mathbf{c_\infty})}\right) = -\frac{\pi^2}{4\mathbf{L}^2}\mathbf{Dt}$$

(16)

Figure 11 shows the result from which D is obtained, knowing the tube length L (~3 cm). In fact this result is not based on the time evolution of c in a single tube. Instead, we have several containers (3 or 4), and holders each containing 6–8 tubes. At time zero, all the holders are each immersed in a different container. At a given time, 2 tubes are removed from two different containers, mixed (in order to attenuate experimental fluctuations) and analyzed by densitometry for their mass fraction c.

We thus have a first way to measure a positive Soret coefficient: From a first experiment in thermogravitational column we get D_T. From a second experiment (the open ended tube) we get D, and
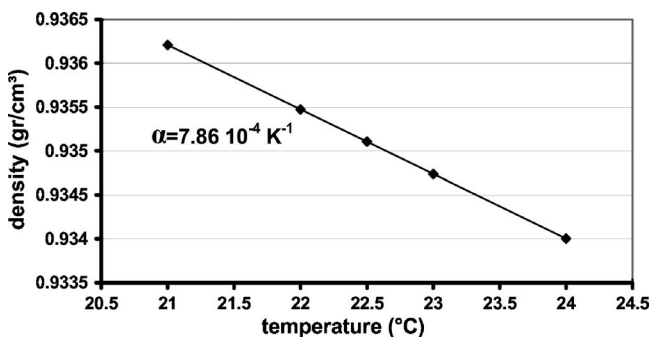
next we calculate the ratio D_T/D. But there is another alternative: The modification of the velocity amplitude followed by laser Doppler velocimetry. Indeed in the same column the heavier component migrates to the cold wall (since $S_T>0$) and the lighter component to the hot wall. Thus the solutal effect adds to the thermal effect to increase the horizontal density gradient and the buoyancy force. Since the amplitude of the vertical velocity component V_a is proportional to the horizontal density gradient

$$\mathbf{V_a} \div \mathbf{g}\frac{\partial\rho}{\partial\mathbf{x}} \div -\alpha\frac{\partial\mathbf{T}}{\partial\mathbf{x}} + \beta\frac{\partial\mathbf{c}}{\partial\mathbf{x}} \div -\alpha\frac{\partial\mathbf{T}}{\partial\mathbf{x}}(\mathbf{1}+\Psi)$$

(17)

it is increased by a factor $(1+\Psi)$ with respect to the thermal effect only. Thus the enhancement of the velocity amplitude is a measure of the separation ratio Ψ, from which S_T is deduced knowing the thermal and mass expansion coefficient given in Figs. 8 and 9. The establishment of the horizontal temperature gradient $\partial T/\partial x$ is a quick process whereas that of the mass fraction gradient $\partial c/\partial x$ is a slow process. But the most important point is that this horizontal mass fraction gradient will almost be destroyed by convection since the component that goes to the cold (resp. to the hot) will be advected to the bottom (resp. to the top), creating a vertical mass fraction gradient $\partial c/\partial z$. In steady-state conditions, the horizontal gradient will not affect the buoyancy force. In other words, the increase in the velocity amplitude is only transitory in time: There is an overshoot phenomenon, nothing more, but this is sufficient to deduce Ψ. Figure 12 shows the time evolution for pure ethanol when at time $t=0$ the thermostats are switched on. Very quickly after 1000 s, the steady state is reached with a velocity amplitude close to 1500 μm/s. There are large fluctuations in the steady value of the velocity; they can be explained as follows: The gap

Fig. 9 Thermal expansion coefficient in the system water (60.88 wt %) – ethanol (39.12 wt %)
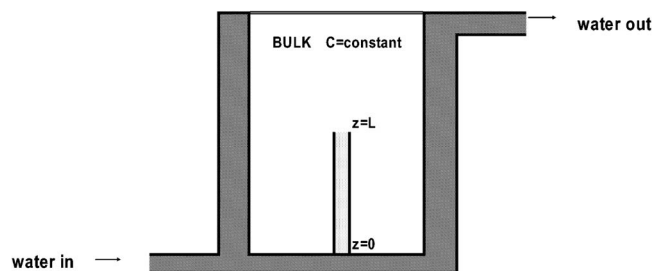

Fig. 10 Sketch of the open ended tube (OET) technique for measuring the isothermal diffusion coefficient
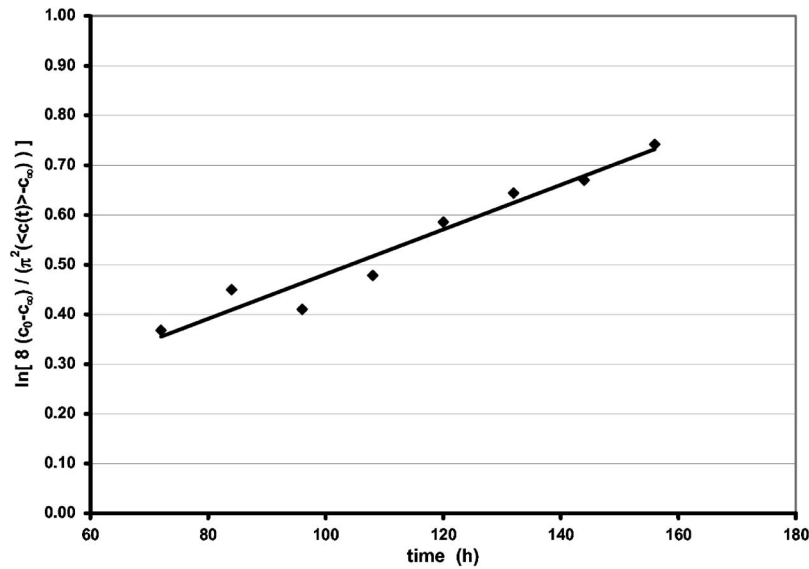
Fig. 11 Time variation of the logarithm of the mean tube concentration in the OET

between the two walls is ~1.6 mm; the raising column is, therefore, 800 μm thick and the velocity raises from zero at the wall to its maximum amplitude in 400 μm. The size of the optical probe in LDV is 90 μm which is not very small compared to the numbers given above. We understand that inside the optical probe there are velocity gradients responsible for the fluctuations. Nevertheless an averaging process for $t > 2000$ s gives the velocity amplitude which can be compared with theoretical predictions, an easy task for a pure substance. Comparison is excellent. For a binary mixture, the time evolution of the velocity amplitude is quite different as shown in Fig. 13 for a mixture of water (50 wt %) and ethanol (50 wt %). A steady-state value is obtained after 4000 s, a time larger than for a pure component. There are still fluctuations due to velocity gradients in the optical probe as explained before. The steady-state value, a little bit less than 300 μm/s is already reached (due to the thermal effect only) after 500 s, a time comparable to that necessary to reach the steady value in a one component system; but in the present case, the velocity continues to increases up to a value close to 380 μm/s, and next drops to the steady value. In order to find with precision the maximum value, excluding fluctuations, we use all the points between $t = 800$ s and $t = 2000$ s, fitted by a cubical polynomial

from which by simple derivation we find the maximum value of the velocity in the least square sense. The relative difference between the maximum velocity and the steady value is a measure of the separation ratio, see Eq. (18), that we call Ψ_{exp}, an "experimental" value, not the real one.

$$\frac{V_a^{max} - V_a^{steady\ st.}}{V_a^{steady\ st.}} = \Psi_{exp} \quad \Psi = \Psi_{exp} \times \tau(H/e, Sc, Gr) \quad (18)$$

In fact in order to find the real value, the experimental value has to be multiplied by a τ corrective factor which accounts for the non-infinite height of the cell. This correction factor τ (greater than one) tends to 1 when H (or better H/e) goes to infinity. Indeed a parcel of fluid raising along the hot wall and coming from the bottom could not have enough time to reach its concentration equilibrium value at the measuring point (the middle of the column) if the column is not high enough. Thus the main parameter in this correction factor is the aspect ratio H/e, but also the relaxation time for diffusion linked to D (or to the Schmidt number Sc in a nondimensional analysis) and the velocity amplitude (or the Grashof number Gr). But we believe that in this review paper this is too much details and interested readers should refer to the original paper [27] for tables of τ values or to [25] for an empirical
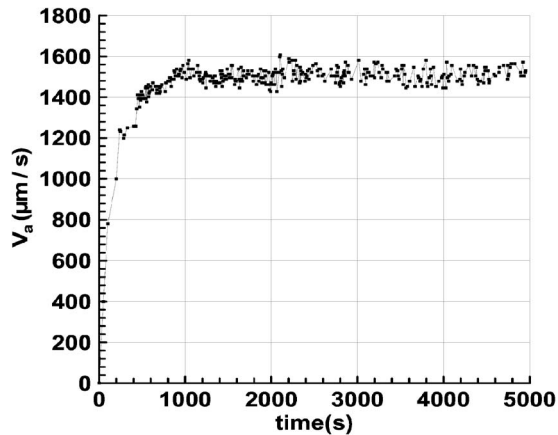

Fig. 12 Time variation of the velocity amplitude in pure ethanol
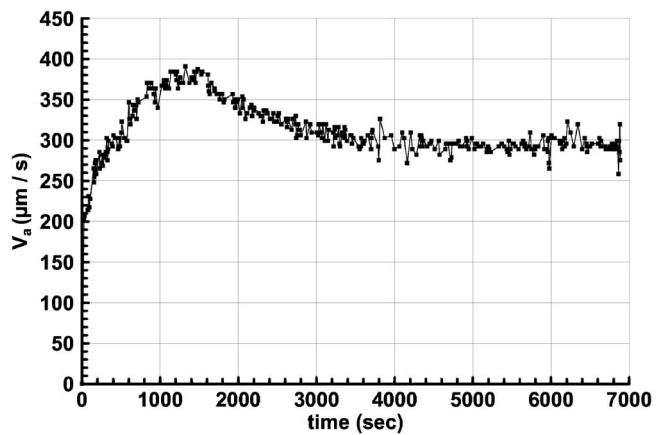

Fig. 13 Time variation of the velocity amplitude in the system water (50 %) – ethanol (50 %)

Table 2 Results for the Soret coefficient based on the overshoot phenomenon in the velocity field observed in thermogravitational columns for the system water (60.88 wt %)–ethanol (39.12 wt %)

Run	V_a^{max} (μm/s)	$V_a^{steady\ st.}$ (μm/s)	Ψ	S_T (10^{-3} K^{-1})
1	228	196	0.193	3.00
2	239	202	0.216	3.36
3	235	200	0.207	3.21
4	234	196	0.229	3.56
		mean value	0.211	3.28
		standard deviation	0.15	0.24
		standard deviation	7%	7%

Table 4 Comparison of the Soret coefficient of the system water (60.88 wt %)–ethanol (39.12 wt %) obtained in different laboratories

Convective coupling [21]	Kolodner [13]	Zhang et al. [14]	Bou-Ali et al. [20]	Köhler and Möller [24]
3.23× 10^{-3} K^{-1}	3.32× 10^{-3} K^{-1}	3.21× 10^{-3} K^{-1}	3.22× 10^{-3} K^{-1}	3.25× 10^{-3} K^{-1}

equation. The experiment is not easy due to the small gap between the walls (1.58 mm) and the difficulty to enter with the laser beam parallel to the wall. In Fig. 13 we have shown the best result that we have for water (50 wt %)–ethanol (50 wt %). Usually the same experiment is repeated four times for each investigated system in order to estimate mean values and standard deviations as well. Table 2 shows the results obtained during the 4 runs for the system water (60.88 wt %)–ethanol (39.12 wt %), a system investigated by many authors.

A standard deviation of 7% is the best that we could obtain with 4 runs using the overshoot phenomenon in the velocity field, Fig. 13. We compare in Table 3 the two methods: Column 1 gives the value of D_T obtained in a first experiment by the 5 samplings along the column height, the analysis of the removed samples and the use of the Furry-Jones-Onsager theory, Eq. (13). Let us note that this value is also the average of several runs. Column 2 is the value of the isothermal diffusion coefficient D by the open ended tube technique and column 3 gives S_T as the ratio of col.1 by col.2. Column 4 reproduces the value of Table 2 for S_T, measuring by LDV the overshoot in the velocity field. The difference between the two values is only 3.4%, and we consider that the mean value of $S_T = 3.23$ 10^{-3} K^{-1} is in some sense the "true" value using convective coupling.

The comparison with other labs is made in [27] with a lot of details, but we give it here for convenience in Table 4. The agreement is simply perfect.

3 The Fontainebleau Benchmark

In view of the different techniques exposed in Sec. 2 and of the results on some water-alcohol mixtures, it seems quite natural to believe that accurate values of the Soret coefficient can be obtained in earth conditions. The E.G.R.T. (European Group of Research in Thermodiffusion) has initiated a project with the aim to provide accurate values for the Soret coefficient for some organic mixtures. During a workshop held at the "Ecole des Mines, Fontainebleau (France)", five European research groups decided to provide a benchmark value for the Soret coefficient for specified mixtures ("The Fontainebleau benchmark"). The participating laboratories are from the universities of Bayreuth, Bilbao, Mons, and Toulouse, and from the Max Planck Institute for Polymer Research in Mainz. The different techniques were already evoked in Sec. 2. Bayreuth and Mainz use the TDFRS technique that allows the simultaneous and independent determination of D, D_T,

and S_T. Bilbao uses the convective coupling in annular thermogravitational columns and by a 2-point sampling process, determines from the mass fraction difference between top and bottom of the column, the thermal diffusion coefficient D_T. Mons in a first experiment determines the time dependent velocity amplitude in a vertical parallelepipedic column (obtained by laser Doppler velocimetry LDV), next uses the five-point sampling process, and finally, in isothermal conditions, the open-ended tube technique to obtain D. In Toulouse, annular thermogravitational columns are also used, but the space between the two cylinders is filled with a porous medium, characterized by its porosity ε and permeability k (packed columns). The Lorenz-Emery theory [33] (a remake of the Fury-Jones-Onsager theory that replaces the Navier-Stokes equation by Darcy's law) is used to deduce D_T. Thus in order to avoid systematic errors, a number of different techniques were employed. In view of a future comparison of these earth results with forthcoming space experiments [34] the five labs have chosen to investigate the mixtures which will fly on the ISS (International Space Station): The three binary mixtures that may be composed with dodecane (C12), isobutylbenzene (IBB), and 1,2,3,4 tetrahydronaphtalene (THN) at a mean temperature of 25°C and 50 wt % in each component. These components have been chosen, as they are representative of a hydrocarbon reservoir mixture, containing (at least when the ternary mixture will be investigated in a next step) an alkane (C12), a one-ring component (IBB) and a two-ring component (THN) [35]. After two years of individual investigations, comparisons between the results produced by each laboratory have been completed and the results published in a common paper accompanied by five individual papers originating from each lab [15,36–40]. The aim of these papers was to propose benchmark values (see Table 5) to which all future techniques should refer. It is our opinion that each new technique, including microgravity experiments, should reproduce these values before gaining confidence.

4 Conclusion

Clearly there is no universal technique that works for measuring the Soret coefficient of any binary mixture. Each technique has its own limitation. As an example, techniques that rely on the variation of index of refraction n with composition c (beam deflection, TDFRS, or simply the analysis of local composition of removed samples based on the measurement of n) will not work near a maximum of n, or at best will be very inaccurate. Also one has to take care of undesired convection currents if the working equations used for deducing S_T from measured quantities are derived for systems at rest. Normally today researchers should be aware of the stability diagram of binary liquid layers initially at

Table 3 Comparison of results for the Soret coefficient based on the overshoot phenomenon in the velocity field and on the vertical mass fraction profile in thermogravitational columns for the system water (60.88 wt %)–ethanol(39.12 wt %)

D_T(10^{-12} m^2 K^{-1}/s) from TGC	D(10^{-10} m^2−s) from OET	S_T(10^{-3} K^{-1}) =col1/col2	S_T(10^{-3} K^{-1}) from LDV	deviation %	$\langle S_T \rangle$(10^{-3} K^{-1}) mean value
1.37	4.32	3.17	3.28	3.4	3.23

Table 5 The Fontainebleau benchmark values for the Soret coefficient of 3 organic liquid mixtures. Initial mass fraction: 50 wt %–50 wt %. C12: dodecane. IBB: isobutylbenzene. THN: tetrahydronaphtalene

			Values of S_T in units 10^{-3} K^{-1}			
Mixture	Mons [28]	Bilbao [29]	Bayreuth [30]	Mainz [31]	Toulouse [32]	Proposed benchmark value [9]
THN-C12	9.98	8.73	9.45	9.52	9.31	9.5 ±0.5
THN-IBB	3.14	3.03	3.46	3.55	3.10	3.3 ±0.3
IBB-C12	3.69	3.96	3.95	3.95		3.9 ±0.1

rest, modified by the Soret effect, including instability of systems heated from above, thought to be stable before 1970: This is the well-known double diffusive convective instability. Also horizontal (lateral) temperature gradients should be avoided in well conducted experiments. Therefore, high resolution laser Doppler velocimetry able to detect velocities down to a few μm/s, should reveal the presence, or not, of these convective currents. Alternatively the LDV technique can be used to catch as carefully as possible the onset of free convection in order to measure the variation of the critical Rayleigh number under the influence of negative separation ratio, from which S_T is deduced. More generally modification of the buoyancy forces due to the Soret effect (at least if density is sensitive to the local composition) will profoundly affect the velocity amplitude. Therefore, measurement of the velocity field is an indirect, but nevertheless not less precise way to have access to the separation ratio. Once again the limitation is due to the sensitivity of the density to compositional variation: Even if the components are quite different in their chemical nature and structure, when their densities are almost equal, buoyancy will not sufficiently change to induce measurable variations of some velocity components. But one has to remain optimistic: All these apparent difficulties are exceptional. And in order to prove that accurate values of the Soret coefficient can be obtained in earth conditions, five European labs decided to investigate independently the same systems, i.e., same chemical compounds from the same batch with the same purity, same composition, and same temperature. After two years of individual work, the comparison of results produced by the different labs showed that this benchmark campaign was a success: The highest difference from the mean was only 7% for one particular system. Therefore, we were able to propose benchmark values and we deny the need sometimes expressed [17] to go to microgravity for measuring Soret coefficients, at least for usual organic mixtures near room temperature. The conclusion could be different for less usual systems like molten salts or metals at higher temperatures.

Before ending this review paper, we should like to mention a recent complementary review by Wiegand [41]. In that paper, the author mainly focused on the optical techniques (rather than on convective coupling) to investigate the thermal diffusion process not only in liquid mixtures, but also in polymer solutions and colloïdal suspensions.

References

[1] Soret, Ch., 1979, "Sur l'état d'équilibre que prend au point de vue de sa concentration une dissolution saline primitivement homohéne dont deux parties sont portées à des températures différentes," Arch. Sci. Phys. Nat., **2**, pp. 48–61.

[2] Ludwig, C., 1856, "Diffusion zwischen ungleich erwwärmten orten gleich zusammengesztzter lösungen," Sitz. Ber. Akad. Wiss. Wien Math-Naturw. Kl., **20**, p. 539.

[3] Soret, Ch., 1880, "Influence de la température sur la distribution des sels dans leurs solutions," Acad. Sci., Paris, C. R., **91**(5), pp. 289–291.

[4] Soret, Ch., 1881, "Sur l'état d'équilibre que prend au point de vue de sa concentration une dissolution saline primitivement homohéne dont deux parties sont portées à des températures différentes," Ann. Chim. Phys., **22**, pp. 293–297.

[5] Weinberger, W., 1964, "The Physics of the Solar Pond," Sol. Energy, **8**, pp. 45–56.

[6] Gregg, M., 1973, "The Microstructure of the Ocean," Sci. Am., **228**, pp. 65–77.

[7] Spiegel, E. A., 1972, "Convection in Stars-II: Special Effects," Annu. Rev. Astron. Astrophys., **10**, pp. 261–304.

[8] Bonner, F. J., and Sundelöf, L. O., 1984, "Thermal Diffusion as a Mechanism for Biological Transport," Z. Naturforsch. C, **39**, pp. 656–661.

[9] Montel, F., 1994, "Importance de la thermodiffusion en exploitation et production pétrolières," Entropie, **184–185**, pp. 86–93.

[10] Montel, F., 1998, "La place de la thermodynamique dans une modélisation des répartitions des espèces d'hydrocarbures dans les réservoirs pétroliers: Incidence sur les problèmes de production," Entropie, **214**, pp. 7–9.

[11] Costesèque, P., El Maâtaoui, M., and Riviere, E., 1994, "Enrichissements sélectif d'dydrocarbures dans les huiles minérales naturelles par diffusion thermogravitationnelle en milieu poreaux et cas des isoméres paraffiniques," Entropie, **184–185**, pp. 94–100.

[12] Costesèque, P., and El Maâtaoui, M., 1994, "Sur la différenciation des hydrocarbures dans les fluids pétroliers par diffusion thermogravitationelle en milieu poreaux en présence d'un contact biphasique huile-eau," Entropie, **184–185**, pp. 101–107.

[13] Costesèque, P., El Maâtaoui, M., and Garrigues, J. C., 1996, "Essai d'analyse des relations entre la mobilité thermodiffusionnelle et les propriétés moléculaires intrinséques des espèces, par la méthode des réseaux de neurones artificiels, dans la cas de mélanges complexes ségrégués par diffusion thermogravitationnelle en milieu poreaux (huiles de gisement)," Entropie, **198–199**, pp. 15–24.

[14] Costesèque, P., Fargue, D., and Jamet, Ph., 2002, "Thermodiffusion in Porous Media and Its Consequences," *Thermal Nonequilibrium Phenomena in Fluid Mixtures* (Lecture Notes in Physics), Springer-Verlag, **584**, pp. 389–427.

[15] Platten, J. K., Bou-Ali, M. M., Costesèque, P., Dutrieux, J. F., Köhler, W. Leppla, C., Wiegand, S., and Wittko, G., 2003, "Benchmark Values for the Soret, Thermal Diffusion and Diffusion Coefficients of Three Binary Organic Liquid Mixtures," Philos. Mag., **83**(17-18), pp. 1965–1971.

[16] Legros, J. C., Goemare, P., and Platten, J. K., 1985, "Soret Coefficient and the Two-Compnoent Benard Convection in the Benzene-Methanol System," Phys. Rev. A, **32**, pp. 1903–1905.

[17] Van Vaerenbergh, S., and Legros, J. Cl., 1998, "Soret Coefficients of Organic Solutions Measured in the Microgravity SCM Experiment and by the Flow and Benard Cells," J. Phys. Chem., **102**, pp. 4426–4431.

[18] Costesèque, P., Pollak, T., Platten, J. K., and Marcoux, M., 2004, "Transient-State Method for Coupled Evaluation of Soret and Fick Coefficients, and Related Tortuosity Factors, Using Free and Porous Packed Thermodiffusion Cells: Application to CuSO4 Aqueous Solution (0.25 M)," Eur. Biophys. J., **15**(3), pp. 249–253.

[19] Kolodner, P., Williams, H., and Moe, C., 1998, "Optical Measurement of the Soret Coefficient of Ethanol/Water Solutions," J. Chem. Phys., **88**(1), pp. 6512–6524.

[20] Zhang, K. J., Briggs, M. E., Gammond, R. W., and Sengers, J. V., 1996, "Optical Measurement of the Soret Coefficient and the Diffusion Coefficient of Liquid Mixtures," J. Chem. Phys., **104**, pp. 6881–6892.

[21] Giglio, M., and Vendramini, A., 1975, "Thermal Diffusion Near a Consolute Critical Point," Phys. Rev. Lett., **34**, pp. 561–564.

[22] Wiegand, S., and Köhler, W., 2002, "Measureemt of Transport Coefficients by an Optical Grating Technique," *Thermal Nonequilibrium Phenomena in Fluid Mixtures* (Lecture Notes in Physics), W. Köhler and S. Wiegand, eds., Springer-Verlag, **584**, pp. 189–210.

[23] Chandrasekhar, S., 1961, *Hydrodynamic and Hydromagnetic Stability*, Oxford University Press, Oxford, UK.

[24] Platten, J. K., Dutrieux, J. F., and Chavepeyer, G., 2002, "Soret Effect and Free Convection: A Way to Measure Soret Coefficients," *Thermal Nonequilibrium Phenomena in Fluid Mixtures* (Lecture Notes in Physics), W. Köhler and S. Wiegand, eds., Springer–Verlag, **584**, pp. 313–333.

[25] Dutrieux, J. F., 2002, "Contribution à la métrologie du coefficient Soret," Ph.D Thesis, University of Mons, Mons, Belgium.

[26] Bou-Ali, M. M., Ecenarro, O., Madariaga, J. A., Santamaria, C., and Valencia, J. J., 1999, "Influence of the Grashof Number on the Stability of the Thermogravitational Effect in Liquid Mixtures With Negative Thermal Diffusion Factors," Entropie, **218-219**, pp. 5–7.

[27] Dutrieux, J. F., Platten, J. K., Chavepeyer, G., and Bou-Ali, M. M., 2002, "On the Measurement of Positive Soret Coefficients," J. Phys. Chem. B, **106**, pp. 6104–6114.

[28] Furry, W. H., Jones, R. C., and Onsager, L., 1939, "On the Theory of Isotope Separation by Thermal Diffusion," Phys. Rev., **55**, pp. 1083–1095.

[29] Jones, R. C., and Furry, W. H., 1946, "The Separation of Isotopes by Thermal Diffusion," Rev. Mod. Phys., **18**(2), pp. 151–224.

[30] Majumdar, S. D., 1951, "The Theory of the Separation of Isotope by Thermal Diffusion," Phys. Rev., **81**(5), pp. 844–848.

[31] Chavepeyer, G., and Platten, J. K., 1996, "Simulation numérique 2D de la séparation dans une colonne de thermogravitation et comparaison avec la théorie de Furry-Jones-Onsager-Majumdar," Entropie, **198-199**, pp. 25–29.

[32] Wakeham, W. A. Nagashima, A., and Sengers, J. V., 1991, "Measurement of the Transport Properties of Fluids," *Experimental Thermodynamics*, Vol. III, Blackwell Scientific Publications, Oxford, UK, Chap. 9.

[33] Lorenz, M., and Emery, A. H., 1995, "The Packed Thermal Diffusion Column," Chem. Phys., **11**, pp. 16–23.

[34] Legros, J. C., Montel, F., Shapiro, A., Caltagirone, J. P., Galieno, G., Agip, De Gieter, P., Dubois, F., Borthaire, L., Istasse, E., and Van Vaerenbergh, S., 2002, *Proceedings of the Fifth International Meeting on Thermodiffusion*, A. Shapiro, ed., University of Denmark, Aug. Lyngby.

[35] Costesèque, P., and Loubet, J. C., 1998, "Influence des concentrations relatives sur la diffusion thermogravitationnelle en milieu poreaux des constituants d'un mélange ternaire d'hydrocarbures (Systéme Dodécane-Isobutylbenzéne-Tétraline)," Entropie, **214**, pp. 53–59.

[36] Platten, J. K., Bou-Ali, M. M., and Dutrieux, J. F., 2003, "Precise Determination of the Soret, Thermodiffusion and Isothermal Diffusion Coefficients of Binary Mixtures of Docecane, Isobutylbenzene and 1,2,3,4-Tetrahydronaphtalene (Contribution of the University of Mons to the Benchmark Test)," Philos. Mag., **83**(17-18), pp. 2001–2010.

[37] Bou-Ali, M. M., Valencia, J. J., Madariaga, J. A., Santamaria, C., Ecenarro, O., and Dutrieux, J. F., 2003, "Determination of the Thermodiffusion Coefficient in Three Binary Orfanic Liquid Mixtures by the Thermogravitational Method (Contribution of the Universitad del País Basco, Bilbao, to the Benchmark Test)," Philos. Mag., **83**(17-18), pp. 2011–2015.

[38] Wittko, G., and Köhler, W., 2003, "Precise Determination of the Soret, Thermal Diffusion and Mass Diffusion Coefficients of Binary Mixtures of Dodecane, Isobutylbanzene and 1,2,3,4-Tetrahydronaphtalene by a Holographic Grating Technique," Philos. Mag., **83**(17-18), pp. 1973–1987.

[39] Leppla, C., and Wiegand, S., 2003, "Investigation of the Soret Effect in Binary Liquid Mixtures by Thermal-Diffusion-Forced Rayleigh Scattering (Contribution to the Benchmark Test)," Philos. Mag., **83**(17-18), pp. 1989–1999.

[40] Costesèque, P., and Loubet, J. C., 2003, "Measuring the Soret Coefficient of Binary Hydrocarbon Mixtures in Packed Thermogravitational Columns (Contribution of Toulouse University tot he Benchmark Test)," Philos. Mag., **83**(17-18), pp. 2017–2022.

[41] Wiegand, S., 2004, "Thermal Diffusion in Liquid Mixtures and Polymer Solutions," J. Phys.: Condens. Matter, **16**, pp. R357–R379.